Published in final edited form as:
Exp Eye Res. 2014 October ; 127: 252–260. doi:10.1016/j.exer.2014.08.006.

Retinal macroglia changes in a triple transgenic mouse model of Alzheimer's disease

Malia M. Edwards[a,*], **José J. Rodríguez**[b,c], **Raquel Gutierrez Lanza**[b], **Joseph Yates**[a], **Alexei Verkhratsky**[b,c,d], and **Gerard A. Lutty**[a]

[a]Wilmer Eye Institute, Johns Hopkins Hospital, M023 Smith Building, 400 N. Broadway, Baltimore, MD 21287, USA

[b]Department of Neurosciences, University of Basque Country, UPV/EHU, Leioa, Spain

[c]IKERBASQUE, Basque Foundation for Science, Bilbao, Spain

[d]Faculty of Life Sciences, The University of Manchester, Oxford Road, Manchester M13 9PT, UK

Abstract

The retinas of Alzheimer's disease (AD) patients and transgenic AD animal models display amyloid beta deposits and degeneration of ganglion cells. Little is known, however, about the glial changes in the AD retina. The present study used a triple transgenic mouse model (3xTG-AD), which carries mutated human amyloid precursor protein, tau, and presenilin 1 genes and closely mimics the human brain pathology, to investigate retinal glial changes in AD. AD cognitive symptoms are known to begin in the 3xTG-AD mice at four months of age but plaques and tangles are not seen until six to twelve months. Müller cells in 3xTG-AD animals were GFAP-positive, indicating activation, at the earliest time point investigated, nine months. Astrocyte activation was also suggested in the 3xTG-AD mice by an apparent increase in size and process number. Another glial marker, S100, was expressed by astrocytes in both the non-transgenic (NTG) controls and 3xTG-AD retinas. Labeling was predominantly nuclear in nine month non-transgenic (NTG) control mice but was also seen in the cytoplasm and processes at 18 months of age. Interestingly, the nuclear localization was not as prominent in the 3xTG-AD retina even at nine months with labeling observed in astrocyte processes. The diffusion of S100 suggests the possible secretion of this protein, as is seen in the brain, with age and, more profoundly, associated with AD. Several dense, abnormally shaped, opaque structures were noted in all 3xTG-AD mice investigated. These structures, which were enveloped by GFAP and S100-positive astrocytes and Müller cells, were positive for amyloid beta, suggesting that they are amyloid plaques. Staining control retinas with amyloid showed similar structures in 30% of NTG animals but these were fewer in number and not associated with glial activation. The results herein indicate retinal glia activation in the 3xTG-AD mouse retina.

[*]Corresponding author. Tel.: +1 410 614 9888; fax: +1 410 955 3447. medwar28@jhmi.edu (M.M. Edwards), j.rodriguez-arellano@ikerbasque.org (J.J. Rodríguez), raquel.gutierrezlanza@gmail.com (R. Gutierrez Lanza), J.R.Yates@exeter.ac.uk (J. Yates), Alexej.Verkhratsky@manchester.ac.uk (A. Verkhratsky), glutty1@jhmi.edu (G.A. Lutty).

The authors have no conflicts of interest to report.

Disclosure statement

All animal studies were approved by University of Manchester and Johns Hopkins University Animal Care and Use Committees.

Keywords

retina; Müller cells; GFAP; astrogliosis; Alzheimer's disease

1. Introduction

Astroglial cells in Alzheimer's disease (AD) undergo complex morphological and functional changes that may contribute to the evolution of this disease (Rodriguez and Verkhratsky, 2011; Rodriguez et al., 2009b; Verkhratsky et al., 2010, 2012). Astrocytes in the AD brain have increased expression of GFAP (Beach and McGeer, 1988), S100B (Marshak et al., 1992), and heme oxygenase 1 (Schipper et al., 2006), while glutamine synthetase is reduced (Robinson, 2001). These changes demonstrate not only the activation of astrocytes but also functional changes. In AD brains, S100B expression is increased in correlation with neuritic plaque density (Mrak et al., 1996; Sheng et al., 1994). Similarly, GFAP expression increases with disease severity (Wharton et al., 2009). This timeline suggests that the astrocyte changes are not simply a response to increases in amyloid beta. Given the dependency of neurons on astrocytes for normal functioning, it is easy to speculate that disruptions to normal astrocyte metabolism or protein expression would affect neurons as well (Steele and Robinson, 2012).

As an extension of the central nervous system, the retina is not spared in AD with patients experiencing optic nerve and ganglion cell degeneration (Blanks et al., 1989, 1996a, 1996b; Hedges et al., 1996; Hinton et al., 1986). In addition, an increase in the ratio of astrocytes to neurons has been noted, although it remains unclear whether this was due to an increase in astrocytes or a reduction of neurons (Blanks et al., 1996b). While some groups have reported amyloid beta plaques in the retina of AD patients (Koronyo-Hamaoui et al., 2011), others have not found plaques (Blanks et al., 1989; Ho et al., 2013). Retinal degeneration and amyloid deposition have also been reported in single and double transgenic models of AD, primarily in the ganglion cell and inner nuclear layers (Liu et al., 2009; Ning et al., 2008; Perez et al., 2009; Shimazawa et al., 2008). Recently, senile plaques in the retina were detected in $APP_{SWE}/PS1\Delta_{E9}$ mice *in vivo*, providing a potential diagnostic tool for AD (Koronyo-Hamaoui et al., 2011). Importantly, in that study, retinal Aβ deposits appeared earlier than those in the brain, suggesting that retinal damage may be an early AD biomarker. Glial changes have also been noted in the retinas of AD patients (Blanks et al., 1996a).

Assuming retinal changes reflect those in the brain, investigation of retina represents a novel, less invasive portal for studying the AD pathology. The retina has the advantage of being readily accessible photographically for *in vivo* diagnosis. In addition, the retina of mouse models can be examined in its entirety *in vivo* or in flatmount postmortem preparations instead of cross sectional analysis needed for the brain.

Here, we extend previous research to investigate changes in retinal glia in a 3xTG-AD mouse model that mimics progression of human AD pathology (Oddo et al., 2003b; Shimazawa et al., 2008). The 3xTG-AD mice, which carry mutated human amyloid precursor protein, tau, and presenilin 1, demonstrate numerous functional impairments

including reduced long term potentiation, altered spatial memory and deficient long-term memory (Oddo et al., 2003a, 2003b). These transgenic mice also show some neuronal loss accompanied by loss of spines on dystrophic dendrites (Bittner et al., 2010). The 3xTG-AD mouse mimics AD pathology more closely than other transgenic AD models (Olabarria et al., 2010).

2. Materials and methods

2.1. Animal generation and care

The 3xTG-AD mice and non-transgenic background-matching controls (NTG) were bred and housed at IKERBASQUE in Bilbao, Spain as previously described (Olabarria et al., 2010; Rodriguez et al., 2008). All animals were used according to ARVO guidelines. Tails from both 3xTG-AD and NTG mice were sent to *Transnetyx* to test for the presence of the retinal degeneration 8 (rd8) mutation in *Crb1*. All tails analyzed were negative for this mutation.

2.2. Tissue collection

All mice were anesthetized by intraperitoneal injection of sodium pentobarbital (50 mg/kg) and perfused with 3.75% acrolein/2% PFA followed by 2% PFA alone as previously described (Olabarria et al., 2010). After perfusion, eyes were enucleated and either washed in phosphate buffer and retinas then dissected or stored in cryopreservation buffer (25% sucrose and 3.5% glycerol in 0.05 M PB at ph 7.4). Tissue was collected from NTG or C57BL/6J controls and 3xTG-AD mice from 9 to 24 months of age (M). A minimum of three control and 3xTG-AD mice were analyzed for each age group.

2.3. Cryopreservation

Whole eyes and fluorescently labeled flatmount retinas were cryopreserved as previously described (Edwards et al., 2011). Briefly, tissues were exposed to increasing concentrations of sucrose, from 5 to 20%, then incubated in 20% sucrose for 2 h, and placed in biopsy molds containing a 2:1 ratio of 20% sucrose to Optimal Cutting Temperature (OCT; Tissuetek/Sakura, Torrance, CA) solution for 30 min. After infiltration, blocks were frozen in isopentane and dry ice. Finally, 8 μm sections were cut using a *Leica* cryostat (Wetzlar, Germany).

2.4. Immunohistochemistry

Flatmounts were used to investigate the GFAP and S100α/β (herein referred to as S100) expression in the retinas of 3xTG-AD and NTG or C57BL/6J mice from 9 to 24 M. Flatmount retinas were blocked in 5% goat serum in Tris-buffered saline (TBS) containing 0.1% BSA and 0.1% Triton ×100 (TBS-T/BSA) for 6 h at 4 °C. Retinas were incubated in a cocktail containing rabbit-anti-GFAP (1:200; Dako, Carpinteria, CA USA) and mouse anti-S100 (1:200; Santa Cruz, Dallas, TX USA) or mouse anti-amyloid beta (1:100; Covance) prepared in 2% goat serum in TBS-T/BSA for 24 h at 4 °C. Following washes, retinas were incubated in fluorescent conjugated secondary antibodies (1:300; goat anti-rabbit cy3 or cy5, goat anti-mouse cy3; Jackson Immunoresearch, West Grove, PA USA), prepared in TBS-T containing $CaCl_2$ for 24 h at 4 °C. Along with secondary antibodies, isolectin from *Griffonia*

simplicifolia (GS isolectin 1:100; Invitrogen, USA) was applied to label retinal vessels. Immunohistochemistry was performed on 8 μm cryosections as previously described (Edwards et al., 2011). In addition to the primary antibodies used for flatmount immunohistochemistry, mouse anti-glutamine synthetase (1:1000; Millipore) was used to label cryosections. Images were taken using a *Zeiss* 710 Meta confocal microscope equipped with *Zen* software (Carl Zeiss, Jena, Germany). A minimum of three mice from each group was analyzed for each antibody.

2.5. Counting of GFAP-positive Müller cells

Müller cells are normally GFAP-negative or express very low levels of this protein (Sarthy et al., 1991) but express this protein upon activation (Eisenfeld et al., 1984; Fisher and Lewis, 2003; Sarthy and Egal, 1995). When imaging a flatmount retina, GFAP-positive Müller cell processes can be seen aligning with the ganglion cell nerve fibers. When imaged at the base of the superficial retinal vessels or below, GFAP-positive Müller cell processes are visible as dots of fluorescence seen throughout the depth of the retina. In order to assess the number of GFAP-positive Müller cell processes (punctate dots), individual images from 20× confocal Z-stacks at the base of the primary retinal vasculature where astrocytes are not in focus (ex. Fig. 1D, H, L, P), were collected from both NTG and 3xTG-AD retinas. Images were opened in Image J software (National Institute of Health, Bethesda, MD USA) and channels split to isolate the GFAP channel. The threshold was then adjusted to accurately represent the number of GFAP-positive Müller cell processes and the image made binary. The “analyze particle” tool with the particle size set at 10–100 and 0–1 circularity was used to count cells. The total number of GFAP-positive cell processes per 20× image was plotted and unpaired *T*-tests used to compare NTG and 3xTG-AD retinas at 9 M and 18–24 M. Images were counted from three animals per group.

3. Results

3.1. Glial activation is noted at 9 M of age in the 3xTG-AD retinas

At 9 M, flatmount analysis revealed astrocytes labeled with GFAP and S100 in both NTG and 3xTG-AD retinas (Fig. 1). The S100 observed in astrocytes of the NTG retinas at 9 M was most intense in the nuclei with a lighter staining in the cytoplasm (Fig. 1A, B, I, J). Cross sectioning of flatmounts also demonstrated labeling of astrocytes (Fig. 1Q). In the 9 M 3xTG-AD retinas, nuclear localization within astrocytes was prominent but cytoplasmic staining was also quite apparent (Fig. 1E, F, M, N). Cytoplasmic staining was particularly strong in the peripapillary region surrounding the optic nerve head (ONH; Fig. 1 E, F) while nuclear staining was strongest in the peripheral retina (Fig. 1N). Cross sectioning of these flatmounts demonstrated S100-positive Müller cell processes as well as nuclei in the 3xTG-AD mice (Fig. 1R). GFAP and GS isolectin co-labeling clearly demonstrated the expected association between astrocytes and blood vessels in both groups (Fig. 1). This was consistent from the ONH and peripapillary region (Fig. 1A, E) to the peripheral retina (Fig. 1I, M). Müller cell processes in this area were also positive for GFAP. In the retina of 3xTG-AD animals, some astrocytes appeared hypertrophic, with increased processes and process length (Fig. 1M, O) compared to that seen in the NTG retinas (Fig. 1I, K).

Punctate GFAP labeling was observed just below the astrocytes in the retinas from 3xTG-AD mice (Fig. 1E, G, M, O) but not the NTG retinas (Fig. 1A, C, I, K). Confocal Z-stack analysis demonstrated that this labeling extended from the inner limiting membrane into the deeper retinal layers. This punctate labeling was best viewed in slices from confocal Z-stacks at the base of the superficial retinal vessels, where astrocytes were no longer in focus (Fig. 1H, P). GFAP-positive punctae could also be observed abutting nerve fibers of the 3xTG-AD retinas, particularly near the optic nerve head (Fig. 1E, G, H). The punctate labeling and extension throughout the retina is consistent with Müller cell processes, which span the retina.

The number of GFAP-positive Müller cell processes in the 3xTG-AD retina was 10-, 15-, and 6-times greater for the optic nerve head area, mid, and peripheral retina, respectively, compared to NTG retinas (Fig. 2). In order to better visualize Müller cells, flatmounts were cryopreserved and sectioned. Cross sectional analysis revealed that GFAP was confined to astrocytes in the NTG retina (Fig. 1S). In the 3xTG-AD retinas, however, Müller cell processes were also GFAP-positive (Fig. 1T).

3.2. Glial activation increased in aged 3xTG-AD mice

Compared to 9 M NTG retinas, S100 labeling of astrocytes in the aged NTG retinas was less nuclear and more diffuse with labeling extending into the cytoplasm (Fig. 3A, B, I, J). Cross sectional analysis confirmed that S100 was limited to astrocytes (Fig. 3Q). The astrocyte processes were even more intensely labeled with S100 in aged 3xTG-AD retinas (Fig. 3E, F, M, N). Cross sectioning of 3xTG-AD flatmount retinas demonstrated the expression of S100 by Müller cells (Fig. 3R). This perspective also showed the diffusion of S100 throughout the retina in the 3xTG-AD retina. Tortuous and disoriented Müller cell processes were also observed with S100 labeling.

As was seen at 9 M, astrocytes were the primary cells labeled with GFAP in the aged (18–24 M) NTG retina (Fig. 3A, C, I, K). The morphology of astrocytes was consistent across the retina and resembled that seen at 9 M. When imaging the deeper focal planes, some GFAP-positive Müller cell processes were also observed (Fig. 3D, L). The number of GFAP-positive Müller cell processes in the aged NTG retinas increased by approximately 2 fold compared to that seen at 9 M (Fig. 2). In the 3xTG-AD retinas, this number was significantly (~10 times) greater (Fig. 2). In fact, the Müller cell labeling was much more prominent than that of astrocytes at this age with endfeet being strongly GFAP-positive (Fig. 3E, G, M, O). In addition, Müller cell processes appeared to extend along the surface of the retina rather than terminating at the ILM. Astrocytes appeared to have more processes in the 3xTG-AD retinas compared to those in the NTG retinas. Cross sectioning of the flatmount retinas further demonstrated the increased number of GFAP-positive Müller cells in 3xTG-AD retinas (Fig. 3T) compared with NTG retinas (Fig. 3S). As was observed in flatmounts, most Müller cells had GFAP labeling throughout their entire radial processes and in endfeet. Cross sections demonstrated that astrocytes and Müller cell endfeet aggregated to form bundles and mats in many areas of the aged 3xTG-AD retinas.

3.3. Glutamine synthetase labeling of Müller cells was unchanged in the retinas of 3xTG-AD mice at 9 M despite activation

The expression of glutamine synthetase, a Müller cell-specific protein, was analyzed in cross sections of 6 M NTG and 9 M 3xTG-AD retinas. In both NTG and 3xTG-AD retinas, glutamine synthetase was present in the entire Müller cell from endfeet to the outer limiting membrane (Supplementary Fig. 1). The staining intensity was similar in all retinas examined.

3.4. Abnormal glial structures were observed in the 3xTG-AD retinas

Clusters of pinkish spots were observed while dissecting 3xTG-AD retinas. Although these spots were prominent at 18–24 M, many smaller spots were also observed in younger 3xTG-AD retinas. Most 3xTG-AD retinas contained at least one of these structures with some containing numerous. No such spots were noted in the control retinas. When imaging immunolabeled retinas, similar shaped structures with a hazy, autofluroescent appearance were noted in the 3xTG-AD retinas at all ages. These irregularly shaped structures were enwrapped in GFAP-positive processes (Fig. 4). Interestingly, some astrocyte processes around these structures extended into the outer retina, as shown by confocal Z-stack slices (Fig. 4A–C). Müller cells positive for GFAP also surrounded these structures while astrocytes had a hypertrophic appearance with an apparent increased number of processes (Figs. 4A–C, 5). Confocal Z-stack analysis demonstrated the depth of these structures and revealed tangles of Müller cells in the outer retina. Cross sectioning of retinas demonstrated that these structures extended into the inner plexiform layer of the retina, well beyond the normal astrocyte localization, and also showed the intense GFAP and S100 labeling surrounding them (Fig. 4D–F).

To better understand the composition of these structures, retinas from 3xTG-AD and control mice were labeled with both GFAP and amyloid beta. In order to verify the amyloid beta staining, retinas from 10 M control mice were incubated in GFAP along with mouse IGg. No labeling was observed with the Mouse IGg at the dilution of the amyloid beta antibody (Fig. 5A–C). Only one of three 10 M control retinas stained with amyloid had deposits. When present, these deposits were not enwrapped in glia (Fig. 5D–F). Numerous amyloid-positive structures were noted in retinas of all 3xTG-AD retinas investigated (Fig. 5G–L). Amyloid deposition varied in size even within a single retina. All areas of amyloid deposition contained GFAP-positive astrocyte and Müller cell processes. Müller cells surrounding deposits were also positive for GFAP.

4. Discussion

Although retinal changes were first observed in AD patients over two decades ago (Blanks et al., 1989, 1996a, 1996b; Hinton et al., 1986), little research has been done to describe this pathology. Recent evidence suggests that retinal pathology may precede that in the brain, potentially providing a biomarker for this disease (Koronyo-Hamaoui et al., 2011). The current study suggests that previously observed neuronal changes are accompanied by glial activation.

Neuroglial cells are fundamental for the pathological progression of AD through multiple reactions, including astrogliosis, astroglial atrophy, and microglial activation (Heneka et al., 2010; Rodriguez et al., 2009a; Rodriguez and Verkhratsky, 2011; Verkhratsky et al., 2010). The data presented herein reveal a retinal gliotic response in the 3xTG-AD mouse model of AD, particularly in Müller cells. Activation of Müller cells, the primary glial cell of the retina, was demonstrated by GFAP and S100 labeling. Müller cells do not normally express these proteins (Sarthy et al., 1991) and GFAP is routinely used as a marker of their activation (Eisenfeld et al., 1984; Fisher and Lewis, 2003; Hirrlinger et al., 2010; Sarthy and Egal, 1995). Activation of protoplasmic retinal astrocytes, however, cannot be assessed as easily because these cells normally express high levels of GFAP.

Many astrocytes within the 3xTG-AD retinas displayed a hypertrophic, reactive morphology. The present study, therefore, supports the earlier report of glial activation in the retinas of AD patients (Blanks et al., 1996a), whereas using the 3xTG-AD mouse model enabled the investigation of different stages of the disease. AD symptoms begin at 9 M in the 3xTG-AD mouse with significant glial changes not noted in the hippocampus around 12–18 M (Olabarria et al., 2010). In the gray matter of the 3xTG-AD mice, however, the earliest glial changes are represented by astroglial atrophy, which became significant at 1 M in the entorhinal cortex, at 6 M in prefrontal cortex, and at 12–18 M in hippocampus (Kulijewicz-Nawrot et al., 2012; Olabarria et al., 2010; Yeh et al., 2011). By contrast, Müller cells and astrocytes showed signs of activation at 9 M (the earliest time point investigated). Therefore, retinal glial activation precedes that in the brain, in the latter gliotic response appears only at later stages and often closely associated with amyloid beta accumulation, especially in the hippocampus (Kulijewicz-Nawrot et al., 2012; Olabarria et al., 2010; Yeh et al., 2011).

While this study focused on macroglia, preliminary studies investigated microglial changes in 3xTG-AD retinas. IBA-1 immunohistochemistry demonstrated some activated microglia (based on morphology) in the 3xTG-AD retinas at 9 M but the majority of these had ramified morphology. The density and morphology of microglia was similar between the two groups. In addition, few microglia were noted in NTG or 3xTG-AD retinas stained with GS isolectin, which labels activated microglia (Fischer et al., 2011). To fully understand microglial activation, however, one must look at the number of dendrites and size of microglia as well as protein markers for activation. It is also important to look at microglia number as this may increase in retinal diseases (Huang et al., 2013) and in the AD brain (Rodriguez et al., 2013). Future studies should also look at microglia in younger animals as microglia may be activated earlier in the disease process.

While glial activation can be a beneficial response to injury, it can also be damaging. Reactive astrocytes and/or Müller cells increase their production of pro-inflammatory cytokines. A prime example of this in AD is the upregulation and release of S100B. At low levels, S100B is neuroprotective, but becomes cytotoxic at higher concentrations (Van Eldik and Wainwright, 2003). In addition, S100B increases the production of Aβ, potentially contributing to plaque formation (Sheng et al., 2000). Cerebrospinal fluid and brain levels of S100B are significantly increased during AD progression (Mrak et al., 1996; Sheng et al., 1996; Van Eldik and Griffin, 1994). The diffuse labeling with S100 and reduced nuclear

localization reported herein may reflect increased secretion of this protein into the AD retina. Further research is required to determine whether retinal astrocytes and Müller cells secrete S100 and what the consequence of this increase in soluble S100 is in the retina.

This study did not observe any changes in glutamine synthetase expression contrary to what is seen in protoplasmic astrocytes in the AD brain. It is important to note, however, that changes in glutamine synthetase in the AD brain are observed mostly in astrocytes associated with amyloid plaques. No potential plaques were noted in the 3xTG-AD retinal sections stained with glutamine synthetase. Therefore, it is possible that reductions in this protein would be noted in Müller cells associated with plaques. Due to a limited supply of animals, glutamine synthetase could not be investigated in the flat perspective in the present study. Also, it is not possible to co-label retinas with amyloid and glutamine synthetase as both antibodies were produced in mouse. These studies would provide the most relevant analysis since glutamine synthetase is reduced in the AD brain in areas surrounding plaques (Olabarria et al., 2011; Robinson, 2001) In addition to the activation of both astrocytes and Müller cells, the analysis of GFAP and S100 labeling demonstrated changes in the morphology of astrocytes across the 3xTG-AD retina compared to controls.

Another finding from the present study is the unusual amyloid-positive structures in the both the 10 M NTG control (33%) and 9 M and older 3xTG-AD retinas (100%). There was no glial response to the amyloid deposits in the control mouse. In the 3xTG-AD retinas of all ages, however, these structures were surrounded by Müller cells and astrocytes intensely labeled with both GFAP and S100. The amyloid appeared to be enwrapped in retinal glia with astrocytes extending beyond their normal localization into the outer retina to fully surround the structures. Müller cells surrounding these deposits were also activated and astrocytes hypertrophic in the 3xTG-AD retinas. This observation supports the previous findings of amyloid plaques in mouse models of AD (Liu et al., 2009; Ning et al., 2008; Perez et al., 2009; Shimazawa et al., 2008).

5. Conclusions

The data presented herein suggest that Müller cells and astrocytes in the AD retina undergo complex remodeling similar to astrocyte changes in the AD brain. Further research is required to fully understand the consequences of the glial activation in the 3xTG-AD retinas and to determine how these changes correlate with any amyloid deposition or tangles. While the 3xTG-AD mouse model is useful for studying AD, it does not exactly mimic AD pathology. Therefore, it is critical to look at the glia in human AD retinas. Determining the correlation between retinal glial changes and amyloid deposition in the retina will also help determine how closely changes in retina mimic those in the brain. The retina provides a useful model for studying AD pathology and treatment efficacy. Furthermore the retina is more easily accessible than the brain and thus can be used for early diagnosis and for further investigations of neuroglial pathology in AD.

Supplementary Material

Refer to Web version on PubMed Central for supplementary material.

Acknowledgments

This research was supported by funding from the Knights Templar Eye Foundation (ME), NEI/NIH EY009357 (GL) and EY01765 (Wilmer), RPB (Wilmer), and AHAF (GL). This study was also supported by an Alzheimer's Research Trust Programme Grant (ART/PG2004A/1) to JJR and AV. Support from the Spanish Government, Plan Nacional de I+D+I 2008-2011 and ISCIII-Sub-dirección General de Evaluación y Fomento de la Investigación (PI10/02738) co-financed by FEDER to JJR and AV and the Government of the Basque Country (AE-2010-1-28, AEGV10/16, GV-2011111020) are also gratefully acknowledged. The authors also thank D. Scott McLeod for assistance with figure preparation.

References

Beach TG, McGeer EG. Lamina-specific arrangement of astrocytic gliosis and senile plaques in Alzheimer's disease visual cortex. Brain Res. 1988; 463:357–361. [PubMed: 3196922]

Bittner T, Fuhrmann M, Burgold S, Ochs SM, Hoffmann N, Mitteregger G, Kretzschmar H, LaFerla FM, Herms J. Multiple events lead to dendritic spine loss in triple transgenic Alzheimer's disease mice. PLoS One. 2010; 5:e15477. [PubMed: 21103384]

Blanks JC, Hinton DR, Sadun AA, Miller CA. Retinal ganglion cell degeneration in Alzheimer's disease. Brain Res. 1989; 501:364–372. [PubMed: 2819446]

Blanks JC, Schmidt SY, Torigoe Y, Porrello KV, Hinton DR, Blanks RH. Retinal pathology in Alzheimer's disease. II Regional neuron loss and glial changes in GCL. Neurobiol Aging. 1996a; 17:385–395. [PubMed: 8725900]

Blanks JC, Torigoe Y, Hinton DR, Blanks RH. Retinal pathology in Alzheimer's disease. I Ganglion cell loss in foveal/parafoveal retina. Neurobiol Aging. 1996b; 17:377–384. [PubMed: 8725899]

Edwards MM, McLeod DS, Grebe R, Heng C, Lefebvre O, Lutty GA. Lama1 mutations lead to vitreoretinal blood vessel formation, persistence of fetal vasculature, and epiretinal membrane formation in mice. BMC Dev Biol. 2011; 11:60. [PubMed: 21999428]

Eisenfeld AJ, Bunt-Milam AH, Sarthy PV. Muller cell expression of glial fibrillary acidic protein after genetic and experimental photoreceptor degeneration in the rat retina. Investig Ophthalmol Vis Sci. 1984; 25:1321–1328. [PubMed: 6386743]

Fischer F, Martin G, Agostini HT. Activation of retinal microglia rather than microglial cell density correlates with retinal neovascularization in the mouse model of oxygen-induced retinopathy. J Neuroinflammation. 2011; 8:120. [PubMed: 21943408]

Fisher SK, Lewis GP. Muller cell and neuronal remodeling in retinal detachment and reattachment and their potential consequences for visual recovery: a review and reconsideration of recent data. Vis Res. 2003; 43:887–897. [PubMed: 12668058]

Hedges TR 3rd, Perez Galves R, Speigelman D, Barbas NR, Peli E, Yardley CJ. Retinal nerve fiber layer abnormalities in Alzheimer's disease. Acta Ophthalmol Scand. 1996; 74:271–275. [PubMed: 8828725]

Heneka MT, Rodriguez JJ, Verkhratsky A. Neuroglia in neurodegeneration. Brain Res Rev. 2010; 63:189–211. [PubMed: 19944719]

Hinton DR, Sadun AA, Blanks JC, Miller CA. Optic-nerve degeneration in Alzheimer's disease. N Engl J Med. 1986; 315:485–487. [PubMed: 3736630]

Hirrlinger PG, Ulbricht E, Iandiev I, Reichenbach A, Pannicke T. Alterations in protein expression and membrane properties during Muller cell gliosis in a murine model of transient retinal ischemia. Neurosci Lett. 2010; 472:73–78. [PubMed: 20132867]

Ho CY, Troncoso JC, Knox D, Stark W, Eberhart CG. Beta-amyloid, phospho-tau and alpha-synuclein deposits similar to those in the brain are not identified in the eyes of Alzheimer's and Parkinson's disease patients. Brain Pathol. 2013

Huang H, Parlier R, Shen JK, Lutty GA, Vinores SA. VEGF receptor blockade markedly reduces retinal microglia/macrophage infiltration into laser-induced CNV. PLoS One. 2013; 8:e71808. [PubMed: 23977149]

Koronyo-Hamaoui M, Koronyo Y, Ljubimov AV, Miller CA, Ko MK, Black KL, Schwartz M, Farkas DL. Identification of amyloid plaques in retinas from Alzheimer's patients and noninvasive in vivo

optical imaging of retinal plaques in a mouse model. Neuroimage. 2011; 54 (Suppl 1):S204–S217. [PubMed: 20550967]

Kulijewicz-Nawrot M, Verkhratsky A, Chvatal A, Sykova E, Rodriguez JJ. Astrocytic cytoskeletal atrophy in the medial prefrontal cortex of a triple transgenic mouse model of Alzheimer's disease. J Anat. 2012; 221:252–262. [PubMed: 22738374]

Liu B, Rasool S, Yang Z, Glabe CG, Schreiber SS, Ge J, Tan Z. Amyloid-peptide vaccinations reduce {beta}-amyloid plaques but exacerbate vascular deposition and inflammation in the retina of Alzheimer's transgenic mice. Am J Pathol. 2009; 175:2099–2110. [PubMed: 19834067]

Marshak DR, Pesce SA, Stanley LC, Griffin WS. Increased S100 beta neurotrophic activity in Alzheimer's disease temporal lobe. Neurobiol Aging. 1992; 13:1–7. [PubMed: 1371849]

Mrak RE, Sheng JG, Griffin WS. Correlation of astrocytic S100 beta expression with dystrophic neurites in amyloid plaques of Alzheimer's disease. J Neuropathol Exp Neurol. 1996; 55:273–279. [PubMed: 8786385]

Ning A, Cui J, To E, Ashe KH, Matsubara J. Amyloid-beta deposits lead to retinal degeneration in a mouse model of Alzheimer disease. Investig Ophthalmol Vis Sci. 2008; 49:5136–5143. [PubMed: 18566467]

Oddo S, Caccamo A, Kitazawa M, Tseng BP, LaFerla FM. Amyloid deposition precedes tangle formation in a triple transgenic model of Alzheimer's disease. Neurobiol Aging. 2003a; 24:1063–1070. [PubMed: 14643377]

Oddo S, Caccamo A, Shepherd JD, Murphy MP, Golde TE, Kayed R, Metherate R, Mattson MP, Akbari Y, LaFerla FM. Triple-transgenic model of Alzheimer's disease with plaques and tangles: intracellular Abeta and synaptic dysfunction. Neuron. 2003b; 39:409–421. [PubMed: 12895417]

Olabarria M, Noristani HN, Verkhratsky A, Rodriguez JJ. Concomitant astroglial atrophy and astrogliosis in a triple transgenic animal model of Alzheimer's disease. Glia. 2010; 58:831–838. [PubMed: 20140958]

Olabarria M, Noristani HN, Verkhratsky A, Rodriguez JJ. Age-dependent decrease in glutamine synthetase expression in the hippocampal astroglia of the triple transgenic Alzheimer's disease mouse model: mechanism for deficient glutamatergic transmission? Mol Neurodegener. 2011; 6:55. [PubMed: 21801442]

Perez SE, Lumayag S, Kovacs B, Mufson EJ, Xu S. Beta-amyloid deposition and functional impairment in the retina of the APPswe/PS1DeltaE9 transgenic mouse model of Alzheimer's disease. Investig Ophthalmol Vis Sci. 2009; 50:793–800. [PubMed: 18791173]

Robinson SR. Changes in the cellular distribution of glutamine synthetase in Alzheimer's disease. J Neurosci Res. 2001; 66:972–980. [PubMed: 11746426]

Rodriguez JJ, Jones VC, Tabuchi M, Allan SM, Knight EM, LaFerla FM, Oddo S, Verkhratsky A. Impaired adult neurogenesis in the dentate gyrus of a triple transgenic mouse model of Alzheimer's disease. PLoS One. 2008; 3:e2935. [PubMed: 18698410]

Rodriguez JJ, Noristani HN, Hilditch T, Olabarria M, Yeh CY, Witton J, Verkhratsky A. Increased densities of resting and activated microglia in the dentate gyrus follow senile plaque formation in the CA1 subfield of the hippocampus in the triple transgenic model of Alzheimer's disease. Neurosci Lett. 2013; 552:129–134. [PubMed: 23827221]

Rodriguez JJ, Olabarria M, Chvatal A, Verkhratsky A. Astroglia in dementia and Alzheimer's disease. Cell Death Differ. 2009a; 16:378–385. [PubMed: 19057621]

Rodriguez JJ, Verkhratsky A. Neuroglial roots of neurodegenerative diseases? Mol Neurobiol. 2011; 43:87–96. [PubMed: 21161612]

Rodriguez MJ, Prats A, Malpesa Y, Andres N, Pugliese M, Batlle M, Mahy N. Pattern of injury with a graded excitotoxic insult and ensuing chronic medial septal damage in the rat brain. J Neurotrauma. 2009b; 26:1823–1834. [PubMed: 19754248]

Sarthy PV, Fu M, Huang J. Developmental expression of the glial fibrillary acidic protein (GFAP) gene in the mouse retina. Cell Mol Neurobiol. 1991; 11:623–637. [PubMed: 1723659]

Sarthy V, Egal H. Transient induction of the glial intermediate filament protein gene in Muller cells in the mouse retina. DNA Cell Biol. 1995; 14:313–320. [PubMed: 7710688]

Schipper HM, Bennett DA, Liberman A, Bienias JL, Schneider JA, Kelly J, Arvanitakis Z. Glial heme oxygenase-1 expression in Alzheimer disease and mild cognitive impairment. Neurobiol Aging. 2006; 27:252–261. [PubMed: 16399210]

Sheng JG, Mrak RE, Bales KR, Cordell B, Paul SM, Jones RA, Woodward S, Zhou XQ, McGinness JM, Griffin WS. Overexpression of the neuritotrophic cytokine S100beta precedes the appearance of neuritic beta-amyloid plaques in APPV717F mice. J Neurochem. 2000; 74:295–301. [PubMed: 10617132]

Sheng JG, Mrak RE, Griffin WS. S100 beta protein expression in Alzheimer disease: potential role in the pathogenesis of neuritic plaques. J Neurosci Res. 1994; 39:398–404. [PubMed: 7884819]

Sheng JG, Mrak RE, Rovnaghi CR, Kozlowska E, Van Eldik LJ, Griffin WS. Human brain S100 beta and S100 beta mRNA expression increases with age: pathogenic implications for Alzheimer's disease. Neurobiol Aging. 1996; 17:359–363. [PubMed: 8725896]

Shimazawa M, Inokuchi Y, Okuno T, Nakajima Y, Sakaguchi G, Kato A, Oku H, Sugiyama T, Kudo T, Ikeda T, Takeda M, Hara H. Reduced retinal function in amyloid precursor protein-over-expressing transgenic mice via attenuating glutamate-N-methyl-d-aspartate receptor signaling. J Neurochem. 2008; 107:279–290. [PubMed: 18691390]

Steele ML, Robinson SR. Reactive astrocytes give neurons less support: implications for Alzheimer's disease. Neurobiol Aging. 2012; 33(423):e421–413.

Van Eldik LJ, Griffin WS. S100 beta expression in Alzheimer's disease: relation to neuropathology in brain regions. Biochim Biophys Acta. 1994; 1223:398–403. [PubMed: 7918676]

Van Eldik LJ, Wainwright MS. The Janus face of glial-derived S100B: beneficial and detrimental functions in the brain. Restor Neurol Neurosci. 2003; 21:97–108. [PubMed: 14530573]

Verkhratsky A, Olabarria M, Noristani HN, Yeh CY, Rodriguez JJ. Astrocytes in Alzheimer's disease. Neurotherapeutics. 2010; 7:399–412. [PubMed: 20880504]

Verkhratsky A, Sofroniew MV, Messing A, deLanerolle NC, Rempe D, Rodriguez JJ, Nedergaard M. Neurological diseases as primary gliopathies: a reassessment of neurocentrism. ASN Neuro. 2012:4.

Wharton SB, O'Callaghan JP, Savva GM, Nicoll JA, Matthews F, Simpson JE, Forster G, Shaw PJ, Brayne C, Ince PG. Population variation in glial fibrillary acidic protein levels in brain ageing: relationship to Alzheimer-type pathology and dementia. Dement Geriatr Cogn Disord. 2009; 27:465–473. [PubMed: 19420941]

Yeh CY, Vadhwana B, Verkhratsky A, Rodriguez JJ. Early astrocytic atrophy in the entorhinal cortex of a triple transgenic animal model of Alzheimer's disease. ASN Neuro. 2011; 3:271–279. [PubMed: 22103264]

Appendix A. Supplementary data

Supplementary data related to this article can be found at http://dx.doi.org/10.1016/j.exer.2014.08.006.

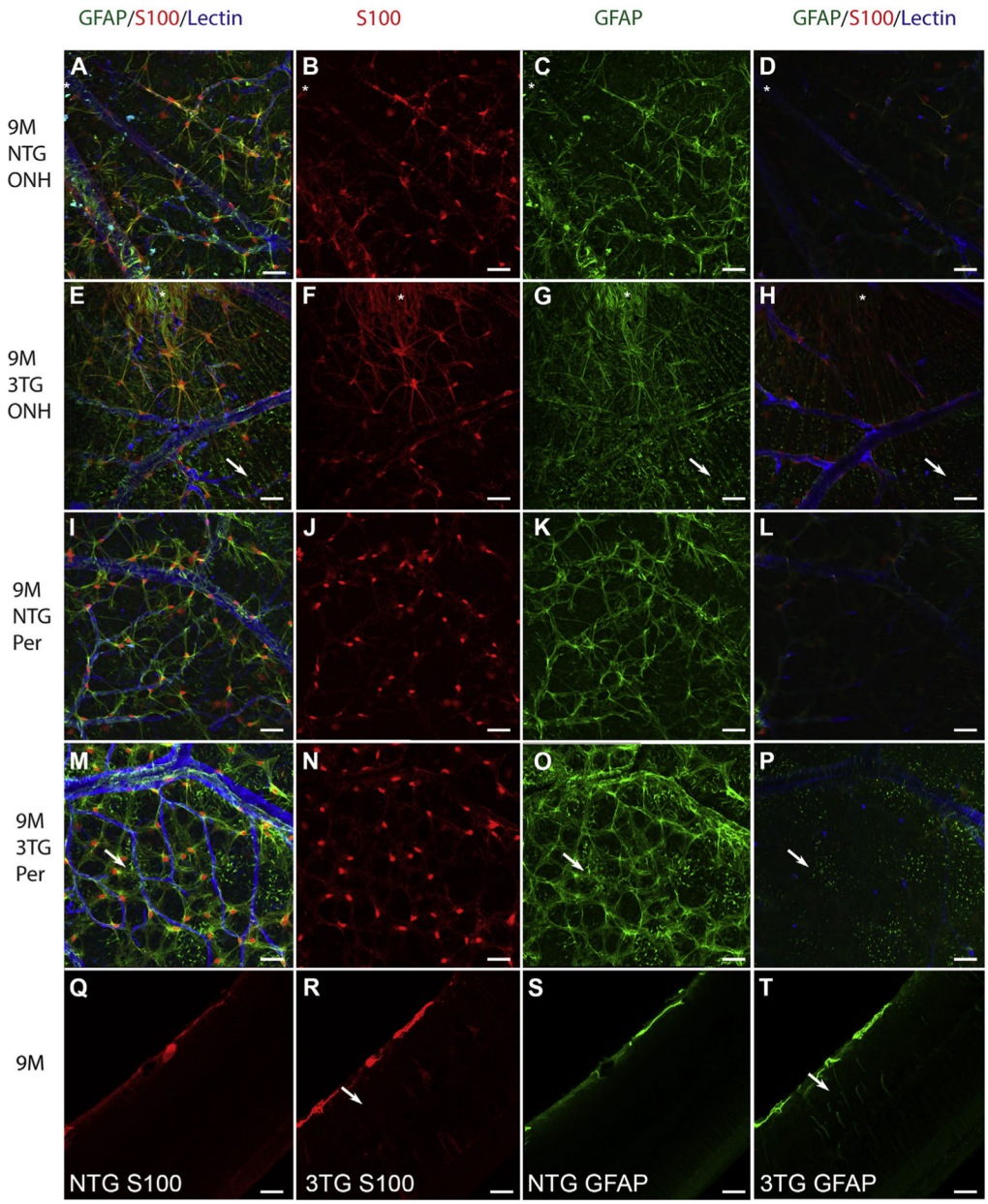

Fig. 1. Glial activation was evident at 9 M in the 3xTG-AD retina

Retinal flatmounts from 9 M NTG (A–D, I–L) and 9 M 3xTG-AD (E–H, M–P) mice were labeled for S100 (red; B, F, J, N), GFAP (green; C, G, K, O), and GS isolectin (blue). S100 was observed primarily in astrocytes with a prominent nuclear stain and some cytoplasmic staining in the NTG retina (B, J). This nuclear staining was slightly less intense in the 3xTG-AD retinas with more labeling of astrocyte processes (F, N). Asterisks indicate the peripapillary region, the area surrounding the ONH in A–H. Arrows indicate GFAP-positive Müller cell processes (E, G, H, M, O, P). Cross section analysis of flatmounts demonstrated that both S100 (Q) and GFAP (S) were confined to astrocytes in the NTG retinas. Müller cells (arrow) were also labeled with both S100 (R) and GFAP (T) in the 3xTG-AD retinas. Scale bars indicate 40 μm.

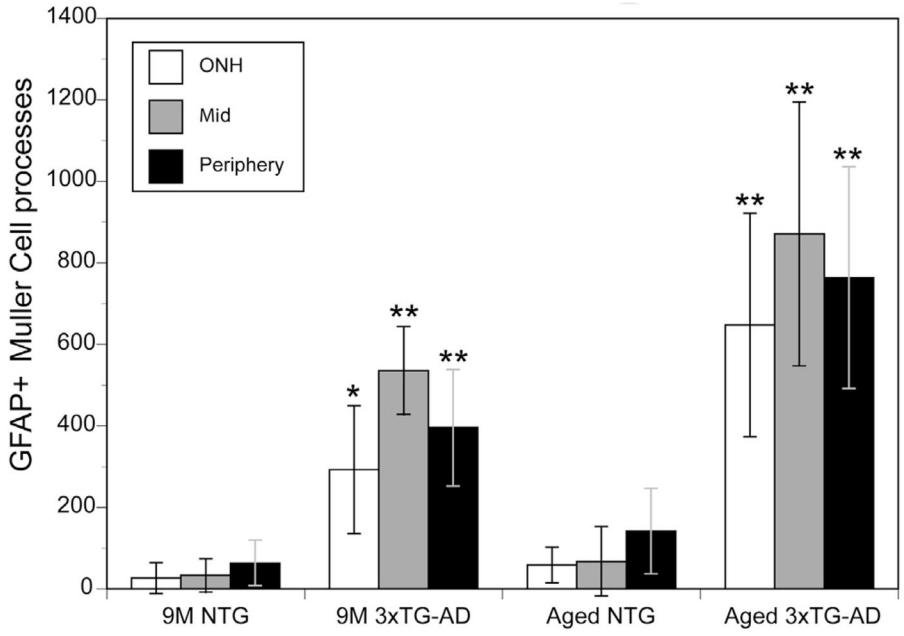

Fig. 2. The number of GFAP-positive Müller cell processes was significantly increased in the 3xTG-AD retina compared to the NTG retina

The average number of GFAP-positive Müller cell processes in a 20× field was counted at the optic nerve head (ONH), mid, and peripheral retina of 9 M and aged (18–24 M) 3xTG-AD and NTG mice. There was a significant increase (*indicates $p < 0.01$, ** indicates $p \leq 0.001$; $n = 3$ per region per group) in all regions of the retina at both time points investigated. Also notable is the slight but non-significant increase in GFAP-positive Müller cells with age observed in the NTG mice. This effect was more drastic, but still not significant, with age in the 3xTG-AD mice.

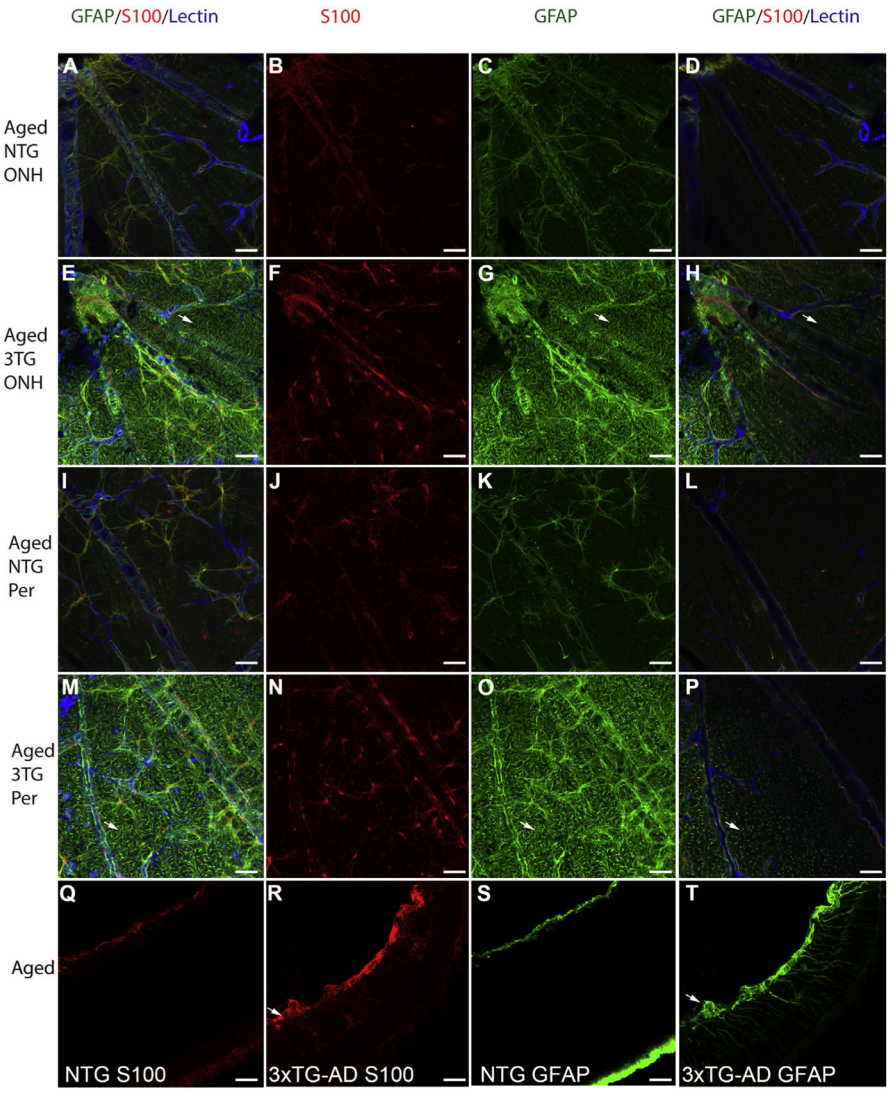

Fig. 3. Müller cell activation is pronounced in the aged 3xTG-AD retina

Retinal flatmounts from aged (18–24 M) NTG (A–D; I–L) and 3xTG-AD (E–H, M–T) mice were labeled for S100 (red; B, F, J, N), GFAP (green; C, G, K, O), and with GS isolectin (blue). In both the optic nerve head area (A–D) and the peripheral retina (I–L), staining in the NTG was confined primarily to astrocytes. S100 labeling extended more into the cytoplasm than at 9 M and the nuclear staining was less intense (B, J). In retina posterior to the superficial vessels, a few GFAP-positive Müller processes were visible (D, L). S100 labeling was more intense and the entire cell was labeled in the aged 3xTG-AD retinas (F, N). Müller cell endfeet could also be seen with S100 staining in these retinas. GFAP-positive Müller cell endfeet appeared dense and enwrapped blood vessels both near the optic nerve (E, G, H) and in the peripheral 3xTG-AD retina (M, O, P). Arrows indicate GFAP-positive Müller cell endfeet in flatmounts. Examination of NTG retinas in the cross sectional perspective, demonstrated that labeling for S100 (Q) and GFAP (S) was confined to astrocytes. By contrast, in the 3xTG-AD retinas S100 (R) and, more drastically, GFAP (T) were observed in the Müller cells as well as astrocytes. Some areas contained dense bundles

(arrow) of S100 and GFAP which appeared to be both astrocytes and Müller cells. Scale bars indicate 40 μm.

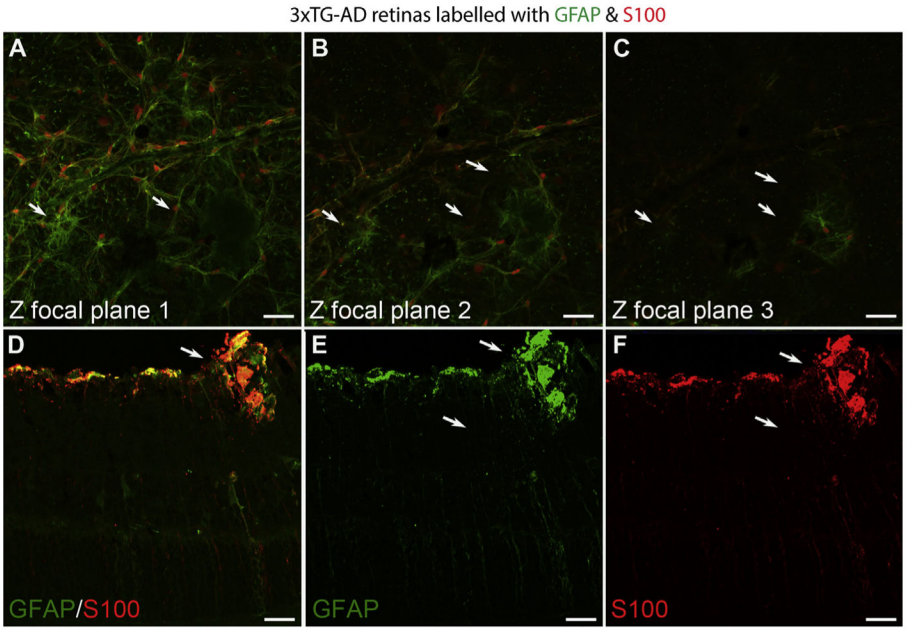

Fig. 4. Abnormal glial structures were observed in 3xTG-AD retinas

Flatmount retinas were labeled for GFAP (green) and S100 (red). Individual Z-stack slices through a 9 M 3xTG-AD retina demonstrate abnormal glial structures (arrows) (A–C). A cross section of a 23 M 3xTG-AD retina stained for GFAP (green, D, E), S100 (red, D, F) demonstrated the density of these structures. Also noted is the activation of Müller cells and astrocytes surrounding these structures. Scale bars indicate 40 μm.

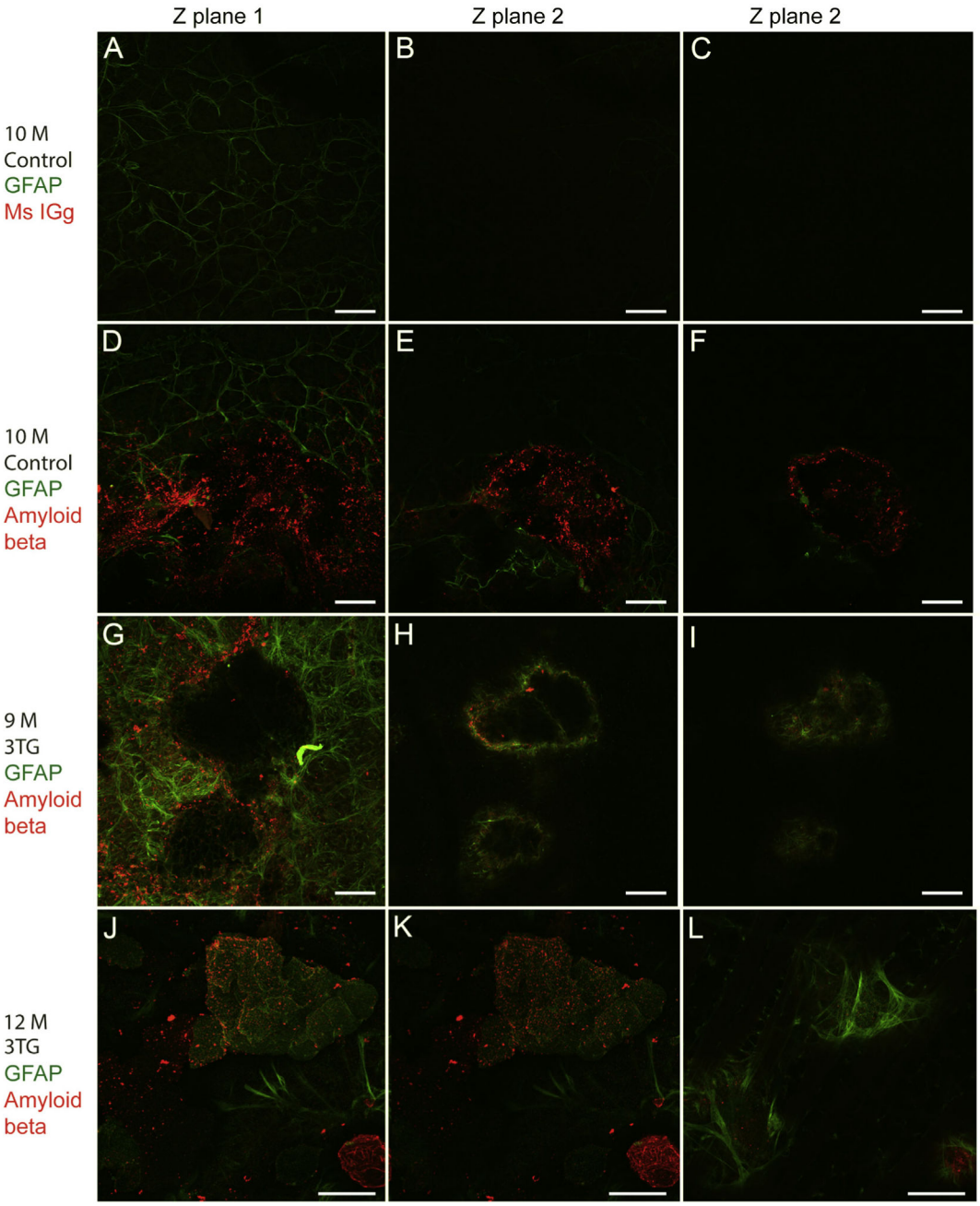

Fig. 5. Glial structures are positive for amyloid beta

Flatmount retinas were labeled for GFAP (green) and amyloid beta or mouse non-immune mouse IgG control (red). Individual slices from confocal Z stacks are shown. Incubation with non-immune Mouse IGg control did not label any structures in the 10 M C57BL/6J retinas (A–C). Some amyloid deposits were found in these 10 M control retinas (D–F). However, there was no activation of astrocytes or Müller cells surrounding these structures. Numerous amyloid deposits were observed in all 3xTG-AD mice investigated, 9 M shown here (G–I). These structures are enwrapped by GFAP-positive glia. The glial ensheathment and activation of Müller cells is better demonstrated at higher magnification (63×) of an

amyloid structure in a 12 M 3xTG-AD retina (J–L). Scale bars indicate: (A–I) 40 μm and (J–L) 30 μm.